Preparation of Reactive Mineral Powders Used for Poly(sodium acrylate) Composite Superabsorbents

Wen-Fu Lee, Yung-Chu Chen

Department of Chemical Engineering, Tatung University, Taipei, Taiwan, Republic of China

Received 6 August 2004; accepted 9 November 2004
DOI 10.1002/app.21812
Published online in Wiley InterScience (www.interscience.wiley.com).

ABSTRACT: Reactive mineral powders were prepared with a vinyl monomer as an intercalating agent, which was grafted onto the surface of nanoclay layers, to offer crosslinking points between the nanoclay layers. According to IR characterization, the vinyl group of (3-acrylamidopropyl)trimethylammonium chloride, grafted onto the clay, disappeared after polymerization was performed. This spectral evidence confirmed that the reaction occurred between the clay layers. Thermogravimetric curves showed that the weight percentage remaining at 750°C for the intercalated clay/sodium acrylate nanocomposites was about 5 wt % higher than that for organic poly(sodium acrylate). This indicated that the clay was not diminished in the polymerization, and this process produced intercalated mica with a quaternary ammonium content of approximately 38.8 mmol/100 g and intercalated montmorillonite with a quaternary ammonium content of approximately 45.36 mmol/100 g. We also investigated the effect of reactive clays on the crystalline morphology and water absorbency for these nanocomposite hydrogels. © 2005 Wiley Periodicals, Inc. J Appl Polym Sci 97: 855–861, 2005

Key words: nanocomposites; superabsorbent; intercalation

INTRODUCTION

Superabsorbents can absorb a large amount of water in comparison with general water-absorbing materials, and the absorbed water is hardly removable even under some pressure. Because of their excellent characteristics, superabsorbents have attracted considerable interest and research and have been used in health, agriculture, and horticulture.[1–4] The first superabsorbent polymer was reported by the U.S. Department of Agriculture in 1961,[5] and many researchers have attempted to modify these absorbent polymers to enhance their absorbency, gel strength, and absorption rate.[6–20]

In recent years, the study of organic–inorganic nanocomposites has become a very important field. Currently, reinforcing polymers with small amounts of smectite clays have been attracting increasing interest because the derived heterostructural materials exhibit impressive mechanical, thermal, optical, and other properties that increase their technological value.[21–26]

Clays have sandwich-type structures with one octahedral Al sheet and two tetrahedral Si sheets and are called philosilicates. There are many types of philosilicates, including kaolinite (KL), montmorillonite (MMT), hectrite, saponite, and mica (MI). Because of their hydrophilic nature, clays are more suitable for use in water absorbents as additives. The components lead to considerable cost reduction.

Hydrotalcite (HT) intercalated with acrylic acid (AA) and 2-acrylamido-2-methyl propane sulfonic acid (AMPS), used to prepare polyacrylate/intercalated HT nanocomposite superabsorbents, has been reported by our laboratory.[27] The intercalation of AA or AMPS into HT makes the HT nanolayers more hydrophilic, enabling them to be exfoliated by acrylate molecules and to generate exfoliated polyacrylate/intercalated hydrotalcite (IHT) nanocomposite hydrogels. Another important reason for the intercalation of AA or AMPS as the intercalated species is to provide a compatible organic/inorganic nanocomposite through the reaction between the vinyl groups of the intercalated IHT and the vinyl groups of the acrylate monomers and to make exfoliated polyacrylate/IHT nanocomposite more compatible. Consequently, exfoliated polyacrylate/IHT nanocomposites with excellent compatibility are expected to show dramatically improved water absorbency and absorption rates over those of pristine polyacrylate. In our studies and many references, the influence of the kind of clay[28] and the effect of intercalating agents[29] on the water absorbency of nanocomposite superabsorbents have been investigated. Wu et al.[28] reported clay/starch-*graft*-polyacrylamide nanocomposites. Their basic idea for

Correspondence to: W.-F. Lee (wflee@ttu.edu.tw).
Contract grant sponsor: National Science Council of the Republic of China; contract grant number: NSC 92-2216-E-036-002.

producing clay/starch-*graft*-polyacrylamide nanocomposites was synthesis through the graft copolymerization reaction of acrylamide, potato starch, and clay mineral powder for reducing the production costs and improving the comprehensive water-absorbing properties of superabsorbent materials.

The inorganic and organic phases are quite incompatible, and this results in phase separation. Thus, interfacial adhesion is introduced between the inorganic and organic components to minimize the degree of phase separation.[30] Generally, the existence of interfacial bonding, especially covalent bonding, between the inorganic and organic phases dramatically improves the mechanical properties.[31] Therefore, the surface of the inorganic components is organically modified before the inorganic/polymer nanocomposites are prepared to enhance the compatibility between the inorganic and organic phases. Furthermore, the organic modification enables the inorganic components to disperse in the polymer matrix. Therefore, the aggregated inorganic components do not form in the polymer matrix, and inorganic/polymer nanocomposites are formed. In summary, the hydrophilic organic modification of the inorganic components is the most important process before clay/poly(sodium acrylate) [poly(NaA)] nanocomposite hydrogels are prepared.

Many reports[32,33] about the intercalation of hydrophobic organic cations into clays have been published, but no reports have discussed the intercalation of hydrophilic organic cations into clays. In this study, the method for preparing organically modified clays differs from conventional methods. Conventional methods incorporate a hydrophobic monomer into clays at higher temperatures.[32,33] Our basic idea for producing the reactive minerals is as follows. The reactive minerals are synthesized by the incorporation of a hydrophilic vinyl monomer into clays at lower temperatures in the first step, and this is followed by polymerization in the interlayer galleries of the clays. Thus, this study also examines the influence of reactive mineral powders for preparing polyacrylate/clay nanocomposite superabsorbents; in addition, the effect of reactive mineral powders on the water absorbency of the nanocomposite superabsorbents has been investigated.

EXPERIMENTAL

Materials

AA, which was purified by vacuum distillation at 63°C and 25 mmHg, and *N,N*′-methylene bisacrylamide (NMBA) as a crosslinking agent were obtained from Aldrich Co. (St. Louis, MO). Diethoxyacetophenone (DEAP) as a photoinitiator was purchased from Fluka Chemical Co. (Buchs, Switzerland). Sodium hydroxide, (3-acrylamidopropyl)trimethylammonium chloride (TMAACl) purchased from Tokyo Kasei Industries, Ltd. (Tokyo, Japan), and NMBA were used directly. MI was purchased from Wako Pure Chemical Industries, Ltd. (Osaka, Japan). KL was purchased from Showa Chemical Industries, Ltd. (Tokyo, Japan). The cation-exchange capacities of MI, KL, and MMT were about 80, 5, and 120 mequiv/100 g, respectively. 4,4′-Azobis(4-cyanovaleric acid) (ACVA), used as an initiator, and sorbitan monostearate (Span 60), used as a stabilizer, were also purchased from Tokyo Kasei Industries. The methanol and cyclohexane were reagent-grade.

Preparation of the sodium acrylate (NaA) monomer solution

We prepared the NaA monomer by gently dropping 6.38 g of a sodium hydroxide solution into 15.32 g of AA under cooling (ice bath). The acid–base reaction was potentiometrically monitored to achieve a degree of neutralization of 75%.

Preparation of the reactive mineral powder

Quaternary alkylammonium-exchanged MI, MMT, and KL were synthesized as follows. The suspension solution, containing 5 g of K^{+}-MI and 1.09 g of TMAACl, 5 g of Na^{+2}-MMT and 1.64 g of TMAACl, or 5 g of KL and 0.069 g of TMAACl, was mixed in 500 mL of water. To protect the vinyl group of TMAACl, the suspension solution was stirred at 30°C for 1 day. Then, the intercalated mineral powder was separated by centrifugation and washed with large volumes of water to remove unreacted TMAACl. The sample was dried in a vacuum oven at 35°C.

Preparation of the NaA and mineral nanocomposite superabsorbent polymer: Inverse suspension polymerization

A 300-mL, four-necked, separable flask equipped with a reflux condenser, a stirring rod, and a thermometer was charged with 65 mL of cyclohexane and 0.2 g of Span 60. The mixture was stirred until Span 60 was dissolved (continuous phase).

The crosslinking agent, NMBA, and the appropriate amount of the intercalated mineral were added to NaA monomer solution, and the mixture was stirred until NMBA was dissolved completely. The monomer solution and 0.15 g of the initiator, ACVA (dispersion phase), were introduced into the reactor. Air was flushed from the reactor by the addition of nitrogen until the entire process was completed. The stirrer speed was maintained at 500 rpm. The polymerization was set at 70°C for 4 h. After polymerization, the suspension solution was cooled and then precipitated with 800 mL of cold methanol under stirring. The

TABLE I
Feed Composition of NaA/Mineral Xerogels Obtained from Inverse Suspension Polymerization

Sample code	Degree of neutralization (%)	NaA (g)	TMAACL–mineral (g)	NMBA (g)	Yield (%)
NaA	75	15	—	0.07	95.4
MI–NaA	75	15	0.789 (5wt%)	0.07	93.5
MI–NaA	75	15	0.789 (5wt%)	0.07	95.6
KL–NaA	75	15	0.789 (5wt%)	0.07	92.7

product was filtered and washed several times with a mixture of water and methanol (1:9 v/v). The product was then dried in a vacuum oven at 100°C for 1 day. A white, powdered polymer was obtained. The feed compositions of the samples are listed in Table I.

Polymerization of the reactive mineral powder

To confirm that the vinyl group of TMAACl that grafted onto the surface of the nanoclay layer was still reactive, intercalated clays in various ratios (intercalated MMT and intercalated MI) and 10 g of water were mixed in a 20-mL sample vial. To this solution, 0.1 wt % DEAP was added, and they were mixed thoroughly. The mixture was then injected into the space between two glass plates with a 2-mm silicone rubber as a spacer. Polymerization was carried out by exposure of the monomer solution to UV irradiation for 20 min. After the gelation was completed, the product was immersed in an excess amount of deionized water for 3 days to remove residual components and dried in a 35°C vacuum oven for 1 day. The products were analyzed by Fourier transform infrared (FTIR) spectra. The yields of the samples are listed in Table II.

FTIR analysis

FTIR spectra were recorded from pressed KBr pellets containing about 1% clay or intercalated clay with a Horiba (Kyoto, Japan) FT/IR-720 spectrophotometer.

TABLE II
Feed Compositions of Intercalated Mineral Clay Solutions Obtained from Photopolymerization

Sample code	Intercalated MMT (IMMT) (g)	Intercalated mica (IMI) (g)	Water (g)	Yield (%)
1 wt % IMMT	0.101	—	10	91.4
2 wt % IMMT	0.204	—	10	94.2
3 wt % IMMT	0.309	—	10	89.4
1 wt % IMI	—	0.101	10	92.9
2 wt % IMI	—	0.204	10	93.3
3 wt % IMI	—	0.309	10	93.4

Thermogravimetric analysis (TGA)

TGA was conducted with a PerkinElmer (Boston, MA) Pyris 1 thermogravimetric analyzer. The experiments were carried out with approximately 4–6-mg samples in flowing air (flow rate = 30 cm^3/min) at a heating rate of 20°C/min.

X-ray diffraction (XRD) analysis

Powder XRD analyses were performed with a Shimadzu (Kanagawa, Japan) model XRD-6000 X-ray powder diffractometer with a Cu anode at 40 kV and 30 mA, with scanning from 2 to 13° at 3°/min. The structure of the mineral was determined at different stages of the nanocomposite synthesis. The mineral powders were mounted on a sample holder with a large cavity, and a smooth surface was obtained by the pressing of the powders with a glass plate. Analyses of the intercalated mineral in the dried gels were performed by the spreading of the mixture on a gel membrane disc (50 mm in diameter and 0.5 mm thick) used as a sample holder. It was designed so that a maximum surface could be irradiated at a low angle; this gave an optimum intensity to the XRD signal. The nanocomposite plates produced during the molding process had a fairly smooth surface.

Measurement of the water absorbency

All samples were dried in a vacuum oven at 100°C before the measurement of the water absorbency. All the samples were used with a particle size in the range of 65–100 mesh.

The samples (50 mg) were immersed in an excess of deionized water for at least 8 h to reach the swelling equilibrium at room temperature, and the residual water was removed by suction filtration with an aspirator (250 mmHg) for 15 min. The gel was weighed, and the equilibrium absorbency (Q_{eq}) was calculated as follows:

$$Q_{eq} = \frac{W_{wet} - W_{dry}}{W_{dry}} \quad (1)$$

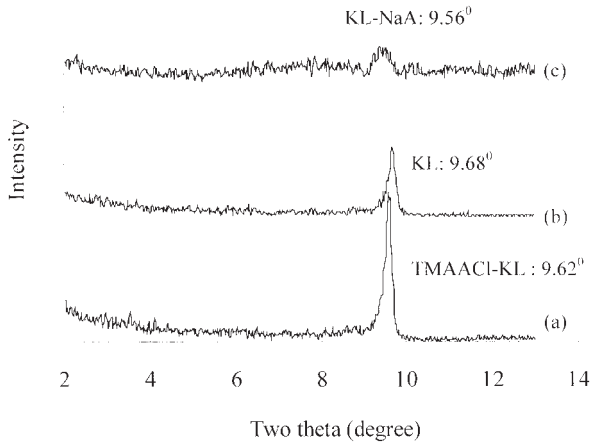

Figure 1 XRD patterns of (a) TMAACl–KL, (b) KL, and (c) KL–NaA.

where W_{dry} is the weight of the dried sample and W_{wet} is the weight of the swollen sample.

RESULTS AND DISCUSSION

Identification of the nanocomposite hydrogels

The XRD patterns of clay, intercalated clay, and nanocomposite gels are plotted in Figures 1–3, respectively. A typical XRD pattern of KL, with a strong peak corresponding to a basal spacing of 9.16 Å, is shown in Figure 1. After intercalation with TMAACl, the peak does not shift to a low angle. This result shows that TMAACl cannot intercalate into the layers of KL during the anion-exchange process; it adopts a lateral layer structure because the cation-exchange capacity of KL is lower than that of MMT and MI. Figure 1 also indicates that the nanocomposite hydrogels show a broad peak at $2\theta = 9.56°$ (d-spacing = 9.27 Å). These results suggest that KL is not easy to intercalate and exfoliate in this system. The XRD pattern of MMT with a strong peak corresponding to a basal spacing of 12.3 Å is shown in Figure 2(a). After intercalation with TMAACl, the peak shifts to a low angle, corresponding to a basal spacing of 15.5 Å [Fig. 2(b)]. A typical diffraction pattern of K^+-MI with a strong peak corresponding to a basal spacing of 9.1 Å can be found in Figure 3(a). After intercalation with TMAACl, this peak shifts to a low angle, corresponding to a basal spacing of 13.5 Å [Fig. 3(b)]. These results indicate that TMAACl ions intercalate the layers of MI and MMT during the cation-exchange process, adopting a lateral bilayer structure. After polymerization with intercalated MI or MMT, the diffraction peaks cannot be observed in Figures 2(c) and 3(c). This suggests that the MI and MMT minerals are exfoliated in poly(NaA/intercalated MI) and poly(NaA/intercalated MMT).

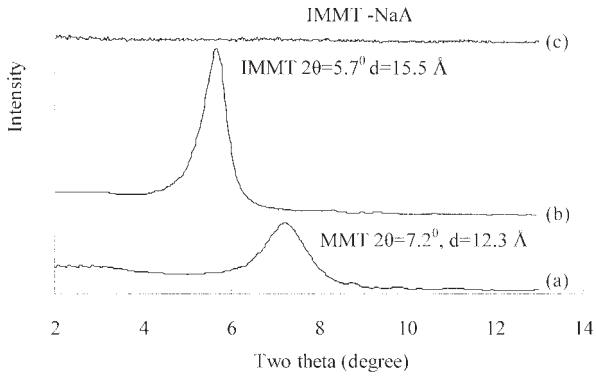

Figure 2 XRD patterns of (a) MMT, (b) IMMT, and (c) IMMT–NaA.

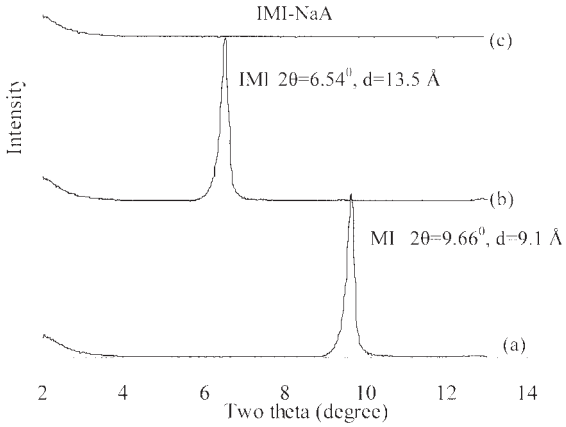

Figure 3 XRD patterns of (a) MI, (b) IMI, and (c) IMI–NaA.

FTIR analysis

Figure 4 shows the FTIR spectra of KL and TMAACl–KL. Figure 4(b) illustrates the tentative IR band assign-

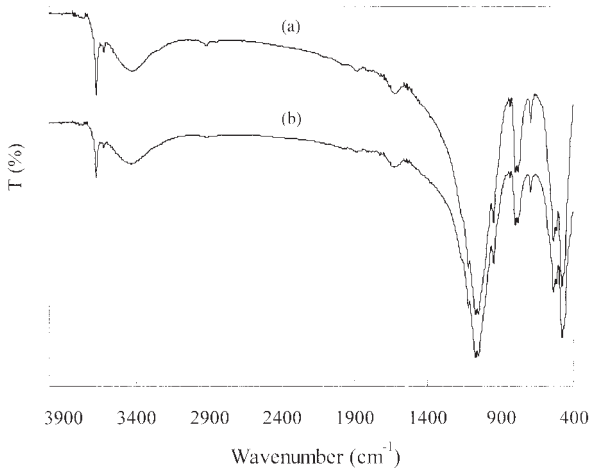

Figure 4 FTIR spectra of (a) KL and (b) intercalated KL.

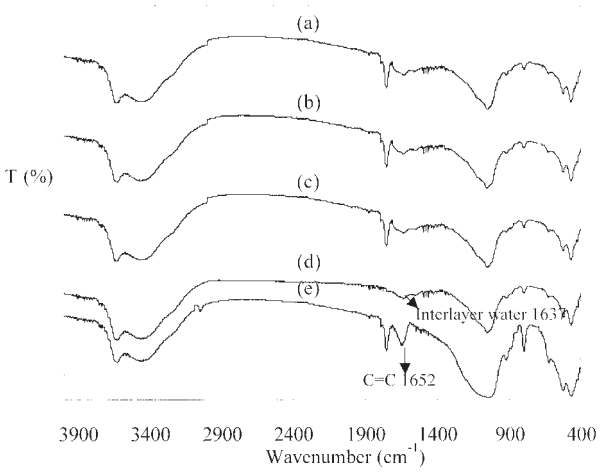

Figure 5 FTIR spectra of (a) 3 wt % IMMT, (b) 2 wt % IMMT, (c) 1 wt % IMMT, (d) MMT, and (e) IMMT.

ments of TMAACl–KL. The characteristic absorption peaks do not appear. This indicates that TMAACl does not intercalate into the KL layers. Figure 5 shows the FTIR spectra of MMT and TMAACl–MMT. The IR absorption band at 1637 cm^{-1} is characteristic of the deformation vibration of the interlayer water of MMT. The band at 3448 cm^{-1} results from the OH stretching vibration of MMT. Additionally, the very strong absorption bands at 1060 cm^{-1} can be ascribed to Si—O stretching vibrations of MMT. The other two strong absorption bands at 802 and 472 cm^{-1} may result from Al—O stretching and Si—O bending vibrations of MMT [see Fig. 5(d)]. Figure 5(e) also illustrates the tentative IR band assignments of TMAACl–MMT. The characteristic absorption peaks of N—H stretching, C═O stretching, and C═C stretching appear at 3650,

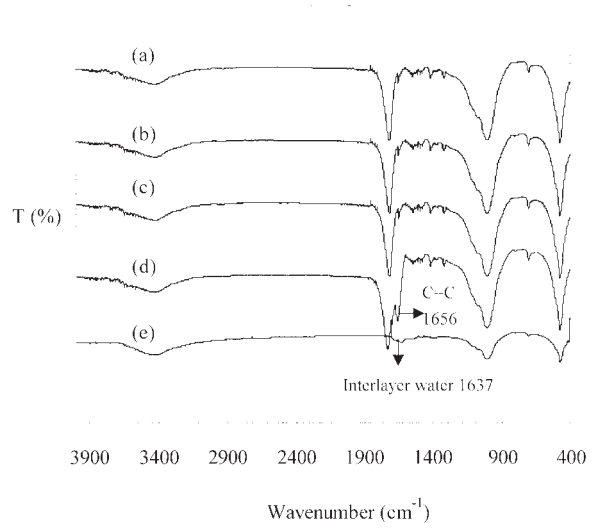

Figure 6 FTIR spectra of (a) 3 wt % IMI, (b) 2 wt % IMI, (c) 1 wt % IMI, (d) IMI, and (e) MI.

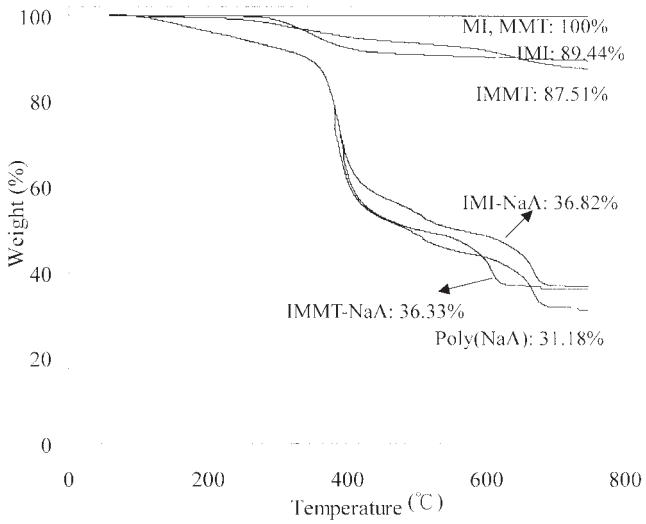

Figure 7 TGA curves of the clay, intercalated clay, and superabsorbent.

1732, and 1652 cm^{-1}, respectively [see Fig. 5(e)]. Figure 6 shows the FTIR spectra of MI and TMAACl–MI. The IR absorption band at 1637 cm^{-1} is characteristic of the deformation vibrations of the interlayer water of MI, as discussed earlier. The band at 3465 cm^{-1} results from the OH stretching vibration of MI. Additionally, the very strong absorption bands at 1016 cm^{-1} can be ascribed to Si—O stretching vibrations of MI. The other two strong absorption bands at 745 and 478 cm^{-1} may have resulted from Al—O stretching and Si—O bending vibrations of MI [see Fig. 6(e)]. Figure 6(d) illustrates tentative IR band assignments of TMAACl–MI. The characteristic absorption peaks of C═O stretching, C═C stretching, CH_2 bending, and CH_3 bending appear at 1718, 1656, 1415, and 1317 cm^{-1}, respectively [see Fig. 6(d)]. The vinyl monomer, TMAACl, that grafts onto the surface of the nanoclay layer can offer reaction points between the nanoclay layer and polymer matrix through *in situ* polymerization. To confirm these results, the effects of different contents of intercalated MI or intercalated MMT through polymerization were investigated. From Figures 4(a–c) and 5(a–c), we know that the vinyl group of TMAACl disappears. Hence, vinyl groups of TMAACl that graft onto the surface of the clay layer react with one another. This spectral evidence confirms that the reaction occurs between the clays and polymer monomer.

Thermal properties of the superabsorbent composites and intercalated clay

Figure 7 shows the dynamic thermogravimetric curves of intercalated clay/NaA nanocomposites with 5 wt % intercalated clay (IMMT and IMI). The decomposition temperatures of these composites are higher

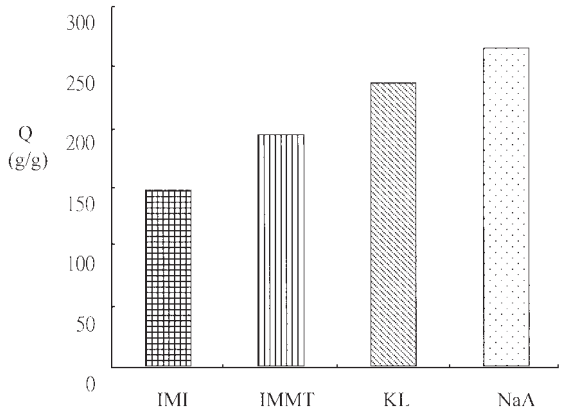

Figure 8 Variation of the absorbency with intercalated MI, intercalated MMT, and KL for poly(NaA)/clay composites with less than 5 wt % clay.

than that of pure poly(NaA). The thermogravimetric curves show that the weight percentage remaining at 750°C for the intercalated clay/NaA nanocomposites is about 5 wt % higher than that of organic poly(NaA) Therefore, the clays are not diminished in polymerization. Thus, the intercalated mineral powder possesses reactivity. Figure 7 also indicates that this process produces intercalated MI with a quaternary ammonium content of approximately 38.8 mmol/100 g and intercalated MMT with a quaternary ammonium content of approximately 45.36 mmol/100 g.

Influence of the mineral powder on the water absorbency of superabsorbents

The type of mineral clay powder is an important factor affecting the absorbent properties of superabsorbent composites. Superabsorbent composites containing KL, intercalated MMT, or intercalated MI powder were prepared under the same conditions. The water absorbency of the three types of superabsorbent composites was measured and is shown in Figure 8.

According to Figure 8, the tendency of the water absorbency for the superabsorbent composites follows the order of KL, intercalated MMT, and intercalated MI in the three types of superabsorbent composites. This may be because the incorporation of the intercalated clay into the gel can enhance the chemical crosslinking between the matrix and dispersed phase. Because the vinyl monomer, TMAACl, grafted onto the surface of the nanoclay layer can offer crosslinking points between the nanoclay layer and polymer matrix through *in situ* polymerization, the compatibility between these two phases can be improved. Thus, the well-dispersed nanoclay layers effectively enhance the gel strength and crosslinking density of the nanocomposites hydrogels.[30] Thus, the absorbency of the composites with pure clay (KL–NaA) is higher than that of the composites with intercalated clay (IMMT–NaA and IMI–NaA) among the superabsorbent composites. Another reason may be that the intercalated MMT and intercalated MI particles exfoliate and disperse on a nanoscale in the gel matrix. This occurrence could increase the particle surface area and result in an increase in the interaction between the gel matrix and intercalated clay dispersed phase.

In addition, Wu et al.[34] suggested that the clay powder could act as an additional network point. Hence, the greater the amount is of the clay powder, the larger the crosslinking density is of the composite. Therefore, the space of the gel network becomes smaller, and the water absorbency gradually decreases. Thus, the absorbency of sodium acrylate is higher than that of the superabsorbent composites (KL–NaA, IMMT–NaA, and IMI–NaA). The hydration ability of MI is lower than that of MMT. Thus, the hydration ability of the layered silicates containing intercalated MMT is higher than that of those containing intercalated MI.[35]

CONCLUSIONS

The following conclusions can be drawn. Reactive minerals can be successfully synthesized by the incorporation of a hydrophilic vinyl monomer into clays at lower temperatures. IR characterization and TGA have confirmed the polymerization reaction of reactive clays and intercalating agents. In addition, the absorbency of composites with KL is higher than that of composites with intercalated MMT, and the absorbency of composites with intercalated MI is lowest of the three types of superabsorbent composites.

References

1. Sakiyama, T.; Chu, C. H.; Fujii, T.; Yano, T. J Appl Polym Sci 1993, 50, 2021.
2. Yoshida, M.; Asano, M.; Kumakura, M. Eur Polym J 1989, 25, 1197.
3. Shiga, T.; Hirose, Y.; Okada, A.; Kurauchi, T. J Appl Polym Sci 1992, 44, 249.
4. Shiga, T.; Hirose, Y.; Okada, A.; Kurauchi, T. J Appl Polym Sci 1993, 47, 113.
5. U.S. Department of Agriculture. U.S. Pat. 3,981,100 (1961).
6. Taylor, N. W.; Fanta, G. F.; Doane, W. M.; Russell, C. R. J Appl Polym Sci 1978, 22, 1343.
7. Burr, R. C.; Fanta, G. F.; Doane, W. M. J Appl Polym Sci 1979, 27, 2713.
8. Fanta, G. F.; Burr, R. C.; Doane, W. M.; Russell, C. R. J Appl Polym Sci 1979, 24, 1384.
9. Kejun, Y.; Berlian, W. J Appl Polym Sci 1990, 41, 3079.
10. Fanta, G. F.; Burr, R. C.; Doane, W. M. J Appl Polym Sci 1979, 24, 2015.
11. Yoshinobu, M.; Morita, M.; Sakata, I. J Appl Polym Sci 1992, 45, 805.
12. Lokhande, H. T.; Varadarjan, P. V.; Iyer, V. J Appl Polym Sci 1992, 45, 2031.
13. Zoda, I. Funct Mater 1986, 6, 76.
14. Isomi, K. Jpn. Pat. 56,707 (1989).

15. Nagasuna, K.; Suminaga, N.; Kimura, K.; Shimonura, T. Jpn. Pat. 126,234 (1989).
16. Imada, H.; Fujiwaka, M. Jpn. Pat. 141,938 (1989).
17. Fujio, A.; Komae, T.; Yutaka, Y. Jpn. Pat. 210,463 (1989).
18. Yada, S.; Shibano, T.; Ito, K. Jpn. Pat. 215,801 (1990).
19. Sano, M.; Mikamo, H.; Suehiro, T.; Wakabayashi, N. Jpn. Pat. 258,839 (1991).
20. Sakiyama, T.; Chu, C. H.; Fujii, T.; Yano, T. J Appl Polym Sci 1993, 50, 2021.
21. Aranda, P.; Ruiz-Hitzky, E. Appl Clay Sci 1999, 15, 119.
22. Giammels, E. P. Adv Mater 1996, 8, 29.
23. Fournaris, K. G.; Karakassides, M. A.; Yiannakopoulou, K.; Petridis, D. Chem Mater 1999, 11, 2372.
24. Kojima, Y.; Usuki, A.; Kawasumi, M.; Okada, A.; Fukushima, Y.; Kurauchi, T.; Kamigaito, O. J Mater Res 1993, 8, 1185.
25. Krishnamoorti, R.; Vaia, R. A.; Giannelis, E. P. Chem Mater 1996, 8, 1728.
26. Lagaly, G. Appl Clay Sci 1999, 15, 1.
27. Lee, W. F.; Chen, Y. C. J Appl Polym Sci, to appear.
28. Wu, J. H.; Lin, J. M.; Zhou, C. R. Macromol Rapid Commun 2000, 21, 1032.
29. Lee, W. F.; Yang, L. G. J Appl Polym Sci 2004, 92, 3422.
30. Mascia, L.; Kioul, A. Polymer 1995, 36, 3646.
31. Tien, Y. I.; Wei, K. H. Macromolecules 2001, 34, 9045.
32. Liang, L.; Liu, J.; Gong, X. Langmuir 2000, 16, 9895.
33. Chen, G. M.; Liu, S. H.; Chen, S. J.; Qi, Z. N. Macromol Chem Phys 2001, 202, 1189.
34. Wu, J. H.; Lin, J. M.; Yang, Z. F.; Pu, M. I. Macromol Rapid Commun 2001, 22, 422.
35. Lee, W. F.; Chen, Y. C. J Appl Polym Sci, submitted.